HHS Public Access

Author manuscript

Proc SPIE Int Soc Opt Eng. Author manuscript; available in PMC 2011 February 04.

Published in final edited form as:

Proc SPIE Int Soc Opt Eng. 2004 ; 5368(2): 534–541. doi:10.1117/12.534568.

Region of Interest (ROI) Computed Tomography

R. Chityala[@,§,†], **K. R. Hoffmann**[§], **D. R. Bednarek**[§,†], and **S. Rudin**[§,†]

[§]Toshiba Stroke Research Center, Rm no: 445, Biomedical Research Building, State University of New York at Buffalo, 3435, Main street, Buffalo, NY, 14214

[†]Erie County Medical Center, 462 Grider Street, Buffalo, NY, 14215

Abstract

High-resolution computed tomography (CT) reconstructions currently require either full field of view (FOV) exposure, resulting in high dose, or region of interest (ROI) exposure, resulting in artifacts. To obtain high-resolution 3D reconstruction of an ROI with minimal artifacts, we have developed a method involving a non-uniform ROI beam filter to reduce dose outside the ROI while acquiring the ROI at a higher dose. High-resolution, high-dose full-field projections of a phantom were obtained. ROIs in the images were selected and the low-dose data outside the ROI were simulated by adding various levels of noise to the projection data corresponding to a dose of 1/16 and 1/256 of the original dose. For an ROI of 30% FOV, artifacts in the reconstructed ROI were minimal for both dose reduction levels. For an ROI of 10% FOV, artifacts remained minimal only for the 1/16th dose case. The effect of the presence of a high contrast object outside the ROI was also studied. We found that the intensity of the artifacts increases with the contrast of the object, its size, and its distance from the axis of rotation. CT using an ROI filter provides a way to reconstruct an ROI with reduced integral dose and yet with minimal artifacts and improved spatial resolution.

Keywords

Region of interest CT; ROI CT; Volume of interest CT; VOI CT; Area of interest CT; Artifact reduction; Dose reduction; reduced FOV; truncated reconstruction

1. INTRODUCTION

Development of high-resolution detectors for Computed Tomography (CT) reconstruction has enabled reconstruction resolution on the order of tens of microns, thus enabling reconstruction of small structures like the cochlea in the inner ear, a stent deployed in a vessel[1], etc. But to achieve high resolution in the reconstruction, the dose required for imaging is very high. To overcome this problem, the area outside the ROI may be blocked by using an x-ray opaque material like lead, reducing the integral dose considerably. Since no data is available outside the ROI, the reconstruction suffers severe artifacts often rendering the image useless. Different approaches have been proposed to reduce these artifacts by estimating data outside the ROI. Lewitt and Bates[2] developed an interpolation

[@]Corresponding author: chityala@buffalo.edu; Tel: 716-829-3595 x114; Fax: 716-829-2212..

technique to determine the truncated data. B. Ohnesorge et al[3], developed an extrapolation procedure which can be incorporated into the convolution step of a filtered back projection. These estimated projections may not model the objects outside the ROI accurately and hence will suffer from artifacts when reconstructed. K. J. Ruchala et al[4], used the *a priori* information from treatment planning CT data in improving the limited field of view (LFOV) reconstruction for online CT systems. But the use of this method is limited to the case in which *a priori* information is available. H. R. Hooper and B. G. Fallone[5] have proposed a method of combining two or more sets of truncated projection data of an object for a fan beam system by merging their sinograms. But this method is limited to fan beam systems and has not been extended for cone-beam systems. A. Faridani et al[6], [7] have proposed a technique called “Local Tomography” which reconstructs using the attenuation measurement along lines very close to the point of interest. But the reconstructed image from local tomography does not represent the map of the attenuation coefficients, but only the edges and boundaries.

In the first part of this paper, we propose an ROI CT technique involving an ROI beam filter[8] to obtain a low dose image outside the ROI and high dose image inside the ROI to obtain reduced artifacts in the reconstructed image. Unlike other methods, no approximations or *a priori* information are required. For this investigation, the low dose data was simulated by adding Gaussian-distributed noise outside the ROI in projection images of a vessel phantom with the ROI remaining unchanged. In the second part of the paper, the effect of an object lying outside the ROI in producing artifacts in the ROI is discussed.

2. ROI RECONSTRUCTION

2.1 Image acquisition

The projection images for the study were acquired using a micro-CT cone-beam system (μCBCT) as shown in Figure 1. The system specification were

1. An x-ray tube from a Bennett MF-1500G Mammography unit, (Bennett X-ray Corporation, Copiague, NY, USA) with a focal spot of 100 microns, 31 kVp, 150 mA and an exposure time of 50 ms.
2. A detector[9] that utilizes a 2D CCD camera and has a field of view (FOV) of approximately 5 cm × 5 cm. The pixel size is 43 microns with an image size of 1024 × 1024 and bit depth of 12.
3. A rotary stage with 0.1 degree precision to acquire images every 2° for a full 360° rotation; thus, 180 projection images are acquired.
4. Vessel phantom constructed using silicon elastomer tube with inner diameter of 3 millimeter. A Tri-Star stent (Guidant Corporation, Indianapolis, IN, USA) was deployed at the neck of the aneurysm. The lumen was filled with a mixture of 50% contrast and 50% solution of water and glycerin mixed 60/40 by volume.
5. A reconstructed volume of 128^3 voxels with an isotropic voxel size of 50 microns.

As indicated in Figure 1, the x-ray source and detector are stationary, and the object is rotated. The projection data acquired from the detector are convolved with the Shepp-Logan filter, after which a Feldkamp reconstruction[10] is performed.

2.2 Low dose simulation

To achieve reduced artifacts in the ROI, we need to obtain low dose data outside the ROI and high dose data in the ROI. This could be accomplished by placing a non-uniform ROI filter in the x-ray beam between the collimator and the object as indicated in Figure 2. In this paper, the dose reduction due to the ROI filter is simulated by increasing the noise level outside the ROI in the projection images.

2.3 Noise and Blur

The dose and relative noise[11] in the projection image are related by the equation

$$\sigma_r^2 \propto 1/dose \quad (1)$$

where $\sigma_r$refers to the relative noise (relative standard deviation) in the image.

In this study, we chose two different dose levels outside the ROI of 1/16 and 1/256 of its original. In both dose levels, the noise level outside the ROI was modified by adding a Gaussian noise of 4 and 16 times its original value.

2.4 Simulation studies

Full FOV projection images of a vessel phantom with an aneurysm in which a stent was placed across the aneurysm neck were obtained. The region corresponding to the ROI was determined, and four different simulations were studied as listed in Table 1. In each of these cases, the region outside the ROI was modified while that inside the ROI was unchanged.

In the first case, the intensity values outside the ROI was set to zero to correspond to a condition when the outside is completely collimated. In the second case, the user indicates the region corresponding to the unattenuated portion in the original image. The average value in this region is taken as the estimated constant value outside the ROI. In the third case, the dose level was 1/16 times its original value, and for the fourth case, the dose level was chosen to be 1/256 times its original value. In all four cases, both a small and a large square-shaped ROI's were studied. The large ROI had a width of 30% of full FOV width and the smaller ROI had a width of 10% of full FOV width.

2.5 Metrics

Qualitative metrics like details visible and the amount of artifact reduced in the reconstructed ROI were used to compare the effectiveness of ROI CT. For quantitative comparison, the difference image between the ROI reconstruction and the full FOV reconstruction was obtained and the root mean square (RMS) value in the difference image within the ROI was calculated in Hounsfield units (HU). The range which is defined as the difference between the maximum and minimum value in the difference image was also obtained in HU.

2.6 Generation of the projection images

The projection images for the four cases as described in section 2.4 were created for ROI reconstruction. Figure 3 shows examples of the projection images. Figure 3a is the full FOV projection image of a vessel phantom. Figure 3b is the simulated projection image for the larger ROI which approximately corresponds to the region shown by the solid square in Figure 3a and Figure 3c is the simulated projection image for the smaller ROI which approximately corresponds to the region shown by the dotted square in Figure 3a. In both cases, the value outside the ROI is set to zero (Case 1 of Table 1). Similar images were generated for the other cases with a constant value outside the ROI and for dose levels of 1/16 and 1/256 outside ROI.

3. EFFECT OF OBJECTS OUTSIDE THE ROI

Objects lying outside the ROI will contribute to artifacts in the ROI during reconstruction because they may be included in a subset of the projections of the ROI. To study the artifacts created by objects outside the ROI and compare it with those obtained for objects in a full FOV reconstruction, we created simulated projection images of a bead. The magnitude of the artifacts was quantified by measuring the standard deviation at the center of the reconstructed images.

For the full FOV reconstruction, the beads were placed at different distances from the center of the image, given different sizes and different levels of contrast and Gaussian noise was added to simulate a real acquisition. These simulated projection images were then used to reconstruct 3D data sets and graphs were plotted showing the relationship between artifacts versus distance, size, and contrast. The FOV for this study was 1.28 centimeter with a pixel size of 50 microns and magnification of 2.

For ROI reconstruction, a 0.5 cm square ROI at the center of image (which is equivalent to 0.125 cm ROI radius on the object plane) was chosen in the full FOV images. The noise outside the ROI was set to correspond to a dose level $1/16^{th}$ of that inside the ROI. The ROI's were reconstructed for different position, size and contrast of the bead and the standard deviation plotted as a function of each parameter. In all the cases, the ROI was empty and the bead was either completely or partly outside the ROI.

4. RESULTS

4.1 Full FOV reconstruction

Figure 4 presents the reconstructed slice obtained with full FOV reconstruction.

4.2 Large ROI

The results for the large ROI are presented in Figure 5. When outside the ROI is set to zero (Figure 5a), high contrast objects like stent wires are discernible but lower in contrast, extended objects like the aneurysm are unclear. When the region outside the ROI was set to the estimated constant value (Figure 5b), artifacts at the edge of the ROI are significantly reduced in comparison to Figure 5a, and the features like the aneurysm are clearly visible. When the dose level outside the ROI was set to 1/256 of its original value (Figure 5c), the

artifacts are further reduced. The RMS difference between this image and the full FOV reconstruction was 8.5 HU, and the range was 45 HU. When the dose level outside the ROI is set to 1/16 of the original value (Figure 5d), the difference between this reconstructed image and the full FOV reconstruction is negligible with an RMS difference of 1.2 HU and a range of 5 HU.

4.3 Small ROI

The results for the small ROI are presented in Figure 6. When the data outside the ROI is set to zero in the projection image, only some of the details like stent wires inside the ROI in the reconstructed image (Figure 6a) are visible due to the artifacts at the edge of the ROI. When the data outside the ROI is set to the estimated value (Figure 6b), the ROI has artifacts. When the dose level outside the ROI is 1/256 of its original value (Figure 6c), the artifacts inside the ROI are further reduced. The RMS difference between the full FOV reconstruction and this ROI reconstruction is 73HU, and the range of the difference image is 120HU. For a dose level outside the ROI 1/16 of the original value (Figure 6d), the quality of the reconstructed image in the ROI is close to that of the full FOV reconstruction (Figure 4). The RMS difference between this image and the full FOV reconstruction is 3.4HU, and the range is 20 HU.

4.4 Non-centered ROI

Displaced detector can be used to increase the area of reconstruction when imaging objects larger than the FOV of the detector. In this scheme, the detector is displaced from the center of the image from 0 to 50% of full FOV size and the truncated images are obtained. Ge Wang[12] has developed a weighting scheme for reconstruction from these truncated images. Similarly, non-centered ROI's (i.e., ROI's whose centers do not match with the center of the projection image) are useful in increasing the size of the ROI in the reconstructed image. But unlike the displaced detector, the data outside are acquired images. We simulated the non-centered ROI in the projection image and reconstructed them for all four conditions (as listed in Table 1) and found a similar quality of reconstruction for the centered and non-centered ROI.

4.5 Effect of objects outside ROI

Figure 7 shows the results following reconstruction of a bead with full FOV projections. It can be seen that the standard deviation of a central region in the reconstructed image (Size = 16 by 16 pixels; 0.8 by 0.8 millimeters) increases with increase in the contrast and size of the object and decreases with the increasing distance of the object from the image center.

Figure 8 shows the results of reconstruction with a bead and an ROI with the dose level outside the ROI corresponding to $1/16^{th}$ of its original. The absolute standard deviation in all three cases increases with increase in the contrast and size of the object and also the distance of the object from the image center.

Thus for full FOV reconstruction (Figure 7), the farther the object, the lesser it contributes to the artifact at the center of the image. This is essentially the result of the back-projection process. But for ROI CT (Figure 8), the farther the object, the more it contributes to the

artifacts at the center of image because the object contributes to a fewer number of projection views as its distance from the center increases.

5. CONCLUSION

From the simulation, it can be seen that for the large ROI in this phantom study even at a dose level of 1/256 outside the ROI, we obtain good quality in the reconstructed image within the ROI. For the large ROI, we obtain good reconstruction even with estimated data (Figure 5b) because the region outside the ROI is relatively uniform, but in general this may not be the case. For a smaller ROI, a dose level of 1/16 results in a reconstructed image close to the full FOV reconstruction. Unlike extrapolation, actual data is acquired outside the ROI and hence the reconstruction will be superior in the case of ROI CT. Also no *a priori* information is required for this technique.

In this paper, we have presented a simulation study for ROI CT whereby the intensity level outside the ROI is the same as that inside. But when data is acquired using an actual ROI beam filter, the data inside and outside the ROI will be at different intensity levels as they are acquired at two different doses and their intensity must be matched[13] prior to back-projection.

For full FOV reconstruction, the objects lying far away from the center of the image result in fewer artifacts at the center of the reconstructed image but for ROI CT, the farther the object, the more it contributes to artifacts. Thus high contrast objects like bone, implants etc lying outside the ROI would results in more artifacts in the reconstructed ROI image hence may limit the use of ROI CT in some applications.

An enhancement of the proposed ROI CT technique could be to perform two scans. One of the scans would be obtained at low dose and with a low resolution full FOV detector and the second scan at a high dose and using a high resolution ROI detector and the two sets of projection data would be fused before reconstruction. An alternate approach could use a hybrid detector that combines high resolution in the ROI and low resolution outside the ROI. In this case, an ROI filter is used to reduce the dose outside the ROI.

In summary, this ROI CT technique helps in

1. Determining the high frequency content in the peripheral areas of the projection image, and hence substantially reducing the artifacts in the reconstructed ROI.
2. Improving the spatial resolution within the reconstructed ROI when used with a high resolution detector in the ROI.
3. Reducing the dose to the patient outside the ROI and
4. Reducing the scattered radiation in the cone-beam projection images.

6. ACKNOWLEDGMENTS

This work was supported by NIH Grant number 1RO1NS38746, 2RO1HLB52567, RO1EB002916, the Toshiba Corporation, the John R. Oishei Foundation and Guidant Corporation.

REFERENCES

1. Chityala, R.; Hoffmann, KR.; Ionita, C.; Rudin, S.; Bednarek, DR.; Wu, Y.; Kyprianou, I. Micro-Cone-Beam CT for Determination of Stent Coverage of Aneurysm Orifice. AAPM 45th annual meeting; San Diego, CA. 2003. p. 1423
2. Lewitt RM, Bates RHT. Image reconstruction from projections. Optik. 1978; 50:Part I, pp. 19, Part II, pp. 85, Part III. pp.189, Part IV, pp. 269.
3. Ohnesorge B, Flohr T, Schwarz K, Heiken JP, Bae KT. Efficient correction for CT image artifacts caused by objects extending outside the scan field of view. Med Phys. Jan; 2000 27(1):39–46. [PubMed: 10659736]
4. Ruchala KJ, Olivera GH, Kapatoes JM, Reckwerdt PJ, Mackie TR. Methods for improving limited field-of-view radiotherapy reconstructions using imperfect *a priori* images. MedPhys. Nov; 2002 29(11):2590–2605.
5. Hooper HR, Fallone BG. Sinogram merging to compensate for truncation of projection data in tomotheraphy imaging. Med Phys. Nov; 2002 29(11):2548–2551. [PubMed: 12462721]
6. Faridani A, Ritman EL, Smith KT. Local Tomography. SIAM. J. Appl. Math. Apr; 1992 52(2):459–484.
7. Faridani A, Ritman EL, Smith KT. Examples of Local Tomography. SIAM. J. Appl. Math. Aug; 1992 52(4):1193–1198.
8. Wagner W. Reconstructions from restricted region scan data – New means to reduce the patient dose. IEEE Transactions on Nuclear Science. Apr.1979 NS-26(2)
9. Rudin, S.; Wu, Y.; Kyprianou, I.; Ionita, C.; Wang, Z.; Ganguly, A.; Bednarek, DR. Proceedings of SPIE 2002: Physics of Medical Imaging. Vol. 4682. SPIE; San Diego, CA: Micro-angiographic detector with fluoroscopic capability; p. 344-353.
10. Feldkamp LA, Davis LC, Kress JW. Practical cone-beam algorithm. J. Opt. Soc. Amer. A. 1984; 6:612–619.
11. Hasegawa, BH. The Physics of Medical X-ray Imaging. Medical Physics publishing; Madison, WI: p. 221
12. Wang, Ge. X-ray micro-CT with a displaced detector array. Med Phys. Jul; 2002 29(7):1634–1636. [PubMed: 12148746]
13. Rudin S, Bednarek DR. Region of interest fluoroscopy. Med Phys. Sep-Oct;1992 19(5):1183–1189. [PubMed: 1435596]

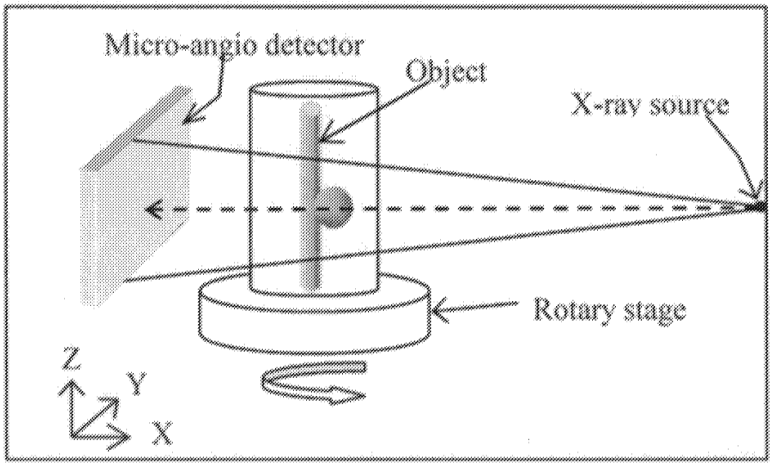

Figure 1.
Schematic of the micro-cone-beam CT setup.

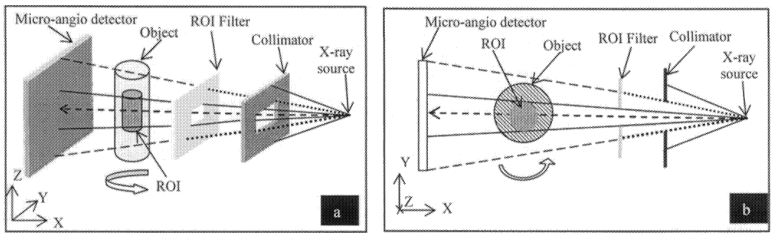

Figure 2.

Schematic of the setup for filtered image acquisition, a) 3D illustration of the ROI filter location b) Top view of the setup.

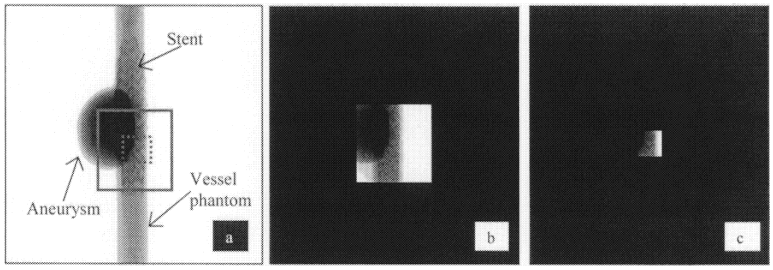

Figure 3.
Actual and simulated projection images, a) Actual full FOV projection image, b) Simulated projection image for large ROI c) Simulated projection image for small ROI.

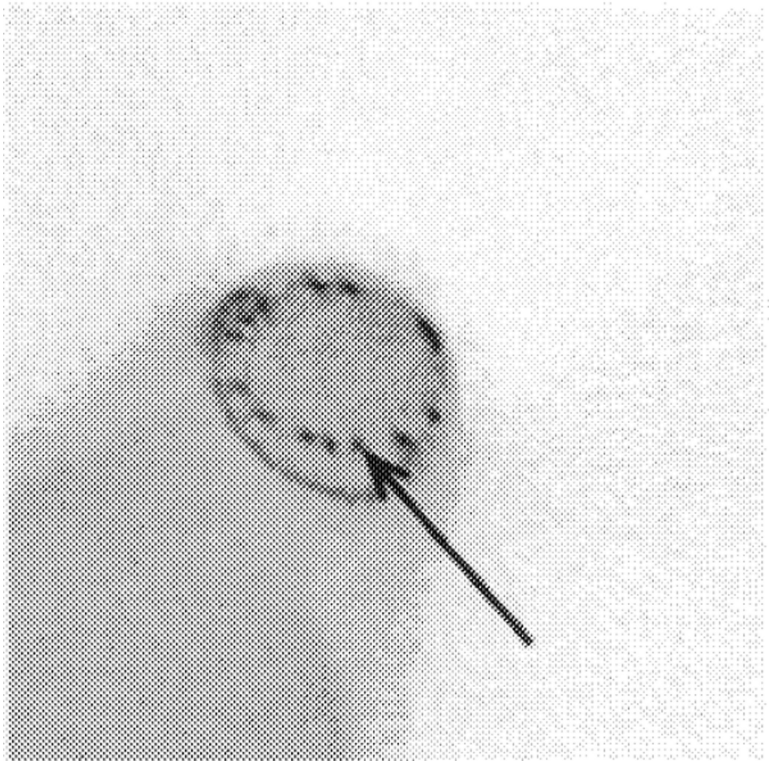

Figure 4.
Full FOV reconstruction. A stent wire is shown by the arrow.

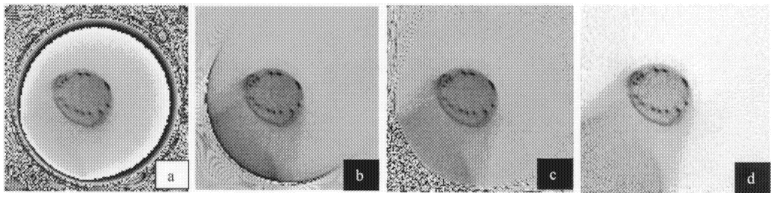

Figure 5.

Reconstructed slices for large ROI. All the four images were normalized to have same window level, a) Outside ROI set to zero in the projection image, b) Outside set to the estimated value, c) Dose level outside ROI = 1/256 of its original value, d) Dose level outside = 1/16 of its original value.

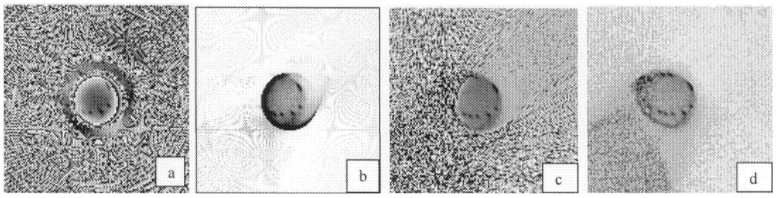

Figure 6.

Reconstructed slices for small ROI. All four images were normalized to have the same window level, a) Outside ROI set to zero in the projection image, b) Outside set to the estimated value, c) Dose level outside ROI = 1/256 of its original value, d) Dose level outside = 1/16 of its original value.

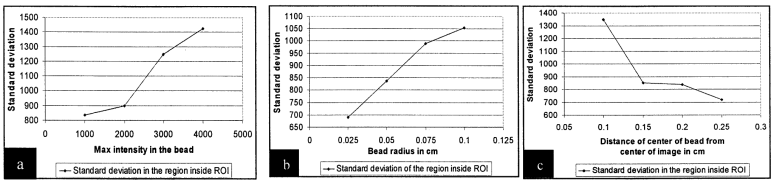

Figure 7.

Standard deviation at the center of the reconstructed image in the full FOV reconstruction as a function of bead a) contrast, b) size, and c) distance from image center.

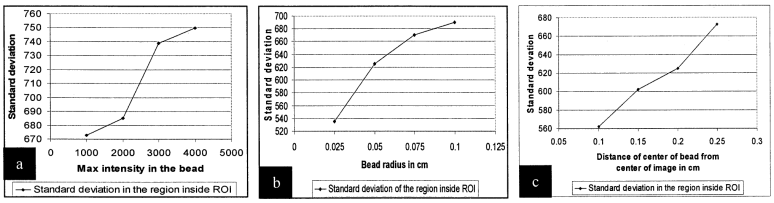

Figure 8.

Standard deviation at the center of the reconstructed image in the ROI reconstruction as a function of bead a) contrast, b) size, and c) distance from image center.

Table 1

Different simulation cases for data outside ROI.

Outside ROI	Simulates condition with
Zero	No data outside ROI
Uniform	Estimated constant value outside ROI
Dose level outside ROI = 1/16 of original value	Low dose acquisition outside ROI.
Dose level outside ROI = 1/256 of original value	Very low dose acquisition outside ROI.